25th Topical Conference on Radio-Frequency Power in Plasmas

Overview of ICRF plasma production and heating in gas mixtures in stellarators

Yu.V. Kovtun[1], V.E. Moiseenko[1,2], H. Kasahara[3], T. Seki[3], R. Seki[3], S. Kamio[4], K. Saito[3], S. Masuzaki[3], M. Yoshinuma[3], D. Hartmann[5], J. Ongena[6], Ye. Kazakov[6], T. Wauters[7], A. Dinklage[5], M. Jakubowski[5], K. Crombé[6], I.E. Garkusha[1]

[1]Institute of Plasma Physics, NSC KIPT, Kharkiv, Ukraine
[2]Ångström Laboratory, Uppsala University, Uppsala, Sweden
[3]National Institute for Fusion Science, Toki, Japan
[4]University of California Irvine, Irvine, CA, United States of America
[5]Max-Planck-Institut für Plasmaphysik, Greifswald, Germany
[6]Laboratory for Plasma Physics, ERM/KMS, Brussels, Belgium
[7]ITER Organization, St. Paul-lez-Durance, France

This work has been carried out within the framework of the EUROfusion Consortium, funded by the European Union via the Euratom Research and Training Programme (Grant Agreement No 101052200 — EUROfusion). Views and opinions expressed are however those of the author(s) only and do not necessarily reflect those of the European Union or the European Commission. Neither the European Union nor the European Commission can be held responsible for them.

19-22 May, 22, 2025 Hohenkammer, Germany

INTRODUCTION

The research of the high temperature plasma for the controlled fusion is essential for the development of magnetic fusion power plant [1].

One of the missions of the EUROfusion consortium’s European research roadmap for the realization of fusion energy is the development of stellarator approach to fusion as a possible long-term alternative to tokamaks [2].

The study of plasma production and heating in the ion cyclotron range of frequencies (ICRF) has a long history in fusion research. The ICRF discharges have been studied in stellarators, tokamaks and mirror devices etc. The scenarios of efficient additional plasma heating using ICRF is one of the main aims of the studies. Plasma production using ICRF discharges is also studied, but to a lesser extent.

1. A. Fasoli, Phys. Rev. Lett. 130, 220001 (2023).
2. K. H. Nordlund, European Research Roadmap to the Realisation of Fusion Energy (2018).

The plasma start-up ICRF

Studies of ICRF plasma production and heating have been carried out in pure hydrogen, deuterium, and helium gases, in the minor regime and in mixtures of these gases.

ICRF discharges for wall conditioning in helium have been studied in the tokamaks TEXTOR-94 [1], Tore Supra [2], HT-7 [3], EAST [4], and JET [5] and in the stellarator W7-AS [6].

The plasma production by ICRF discharges in pure gases has also been studied previously in the CHS [7], W7-AS [8], U-3M [9, 10] and U-2M [10], and LHD [11] stellarators.

1. H. G. Esser, et al, J. Nucl. Mater. 241–243, 861 (1997).
2. E. Gauthier, et al J. Nucl. Mater. 241–243, 553 (1997)
3. J. S. Hu, et al, J. Nucl. Mater 366(1–2), 206 (2007).
4. J. S. Hu, et al J. Nucl. Mater. 376(2), 207 (2008).
5. Y. Kovtun et al, Nucl. Mater. Energy 37, 101521 (2023).
6. Brakel, et al J. Nucl. Mater. 290–293, 1160 (2001).
7. K. Nishimura, et al Fusion Technol. 17(1), 86 (1990).
8. W. Ballico, et al AIP Conf. Proc. 244, 150 (1992).
9. V. E. Moiseenko, et al Plasma Phys. Controlled Fusion 61, 065006 (2019).
10. V. E. Moiseenko, et al Nucl. Fusion 51(8), 083036 (2011).
11. Y. Torii, et al Nucl. Fusion 42(6), 679 (2002)

The plasma start-up ICRF

ICRF discharges in H_2+He mixtures have also been used for wall conditioning in the tokamaks TEXTOR and ASDEX Upgrade. In these experiments, plasma densities in the range of **10^{16}–$5\ 10^{17}$ m^3** were observed [1-4].

The plasma of ICRF discharges in H_2+He mixtures has been studied in Sirius [5] and H-1NF (H-1) stellarators [6]. In H-1NF experiments, densities up to ≈ **$2\ 10^{18}$ m^3** and electron temperatures of several tens of eV have been observed with injected RF power up to 80 kW.

In support of the ICRF experiments for plasma production at Wendelstein 7-X, studies on the development of an ICRF start-up scenario were initiated on the Uragan-2M (U-2M) stellarator. Then, the ICRF plasma production was demonstrated on the LHD with the scenario based on U-2M experiment.

1. A. Lyssoivan, et al J. Nucl. Mater. 337–339, 456 (2005).
2. A. Lyssoivan, et al J. Nucl. Mater. 363–365, 1358 (2007).
3. M. K. Paul, et al AIP Conf. Proc. 1187, 177 (2009).
4. A. Lyssoivan, at el J. Nucl. Mater. 390–391, 907 (2009).
5. P. Y. Burchenko, at el JETP Lett. 15(5), 174 (1972).
6. M. J. Hole, et al Plasma Phys. Controlled Fusion 59(12), 125007 (2017).

ICRF production of plasma in Uragan-2M stellarator

Stellarator Uragan-2M

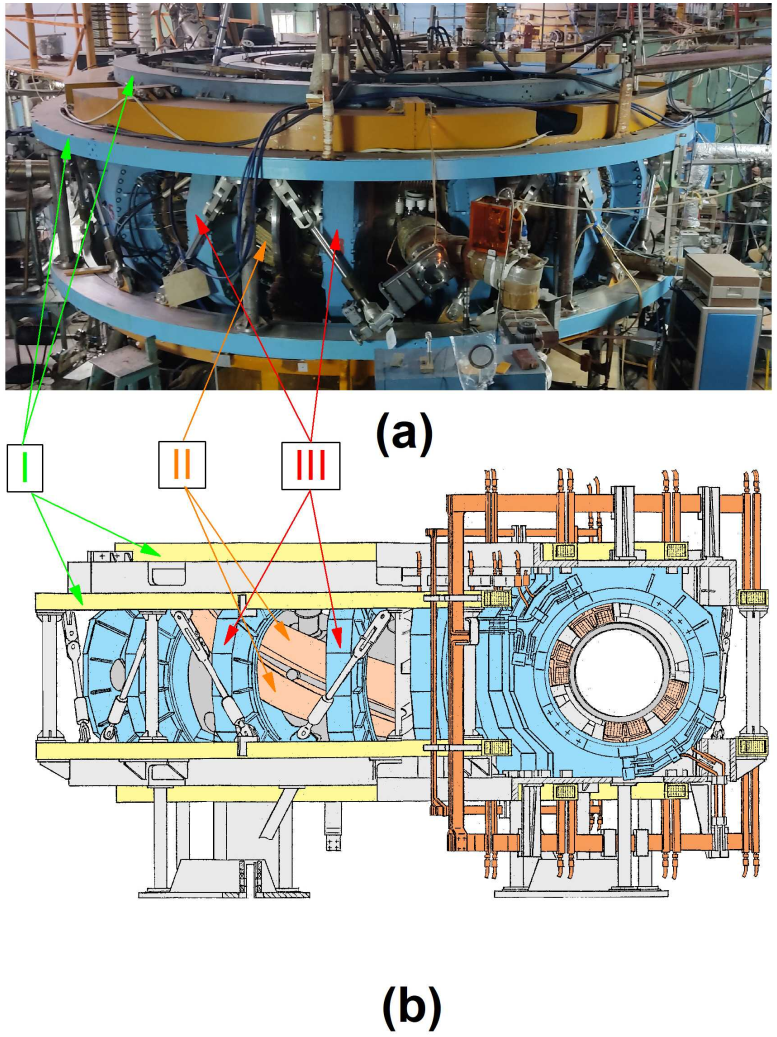

The photo of the U-2M (a), the schematic view of the U-2M (b). I the poloidal field coils; II the helical field coils; III the toroidal field coils.

The Uragan-2M device [1] at Kharkiv, Ukraine, is a medium-size stellarator of the torsatron type.

The U-2M was manufactured and assembled in the early 1990s, was put into operation and briefly exploited, and then conserved [2].

It was partially modernized, and put again to operation at the end of 2006 [3].

Device characteristics	
Major radius, R (m)	**1.7**
Minor radius, r (m)	**0.34**
Plasma volume, V_p (m^3)	**~ 1.6**
Magnetic field, B (T)	**< 0.6 (max 2.4 T)**
Total heating power, (MW)	**< 0.4**
Plasma heating tools	**ICRF**

1. Y.V. Kovtun et al. Fusion Engineering and Design 194 (2023) 113887
2. O. S. Pavlichenko Plasma Phys. Control. Fusion 35 B223 (1993).
3. A. Beletskii et al. Probl. At. Sci. Technol. Ser.: Plasma Phys. 6, 13–15 (2008).

TWO-STRAP RF ANTENNA

(a)

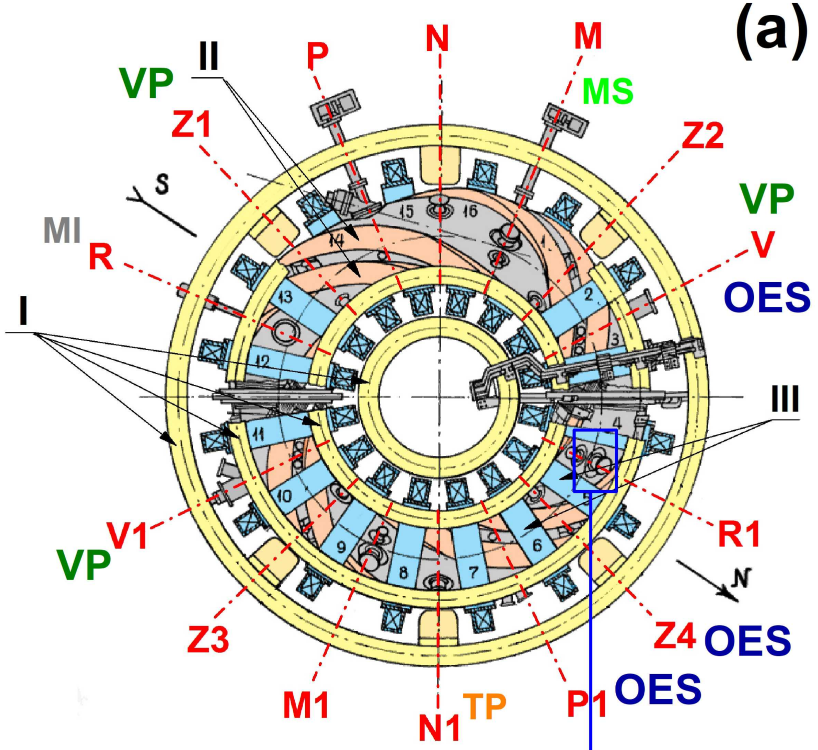

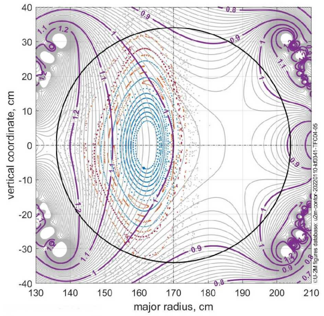

(b)

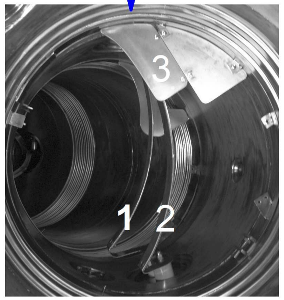

(c)

The two-strap antenna operated in monopole phasing was connected to pulsed RF systems “Kaskad-1” (K-1) [1-3].

The generator operate at a constant frequency in the range of 3–15 MHz.

The pulse duration up to 100 ms.

The maximum output power of the generator is about 0.4 MW.

1. Y.V. Kovtun et al. Fusion Engineering and Design 194 (2023) 113887
2. V. Moiseenko et al. J. Plasma Phys., 86, 905860517 (2020)
3. A.V. Lozin et al., Probl. At. Sci. Technol. Ser.: Plasma Phys. 6, 10-14 (2020).

(a) General view of stellarator Uragan-2M. I the poloidal field coils; II the helical field coils; III the toroidal field coils (numbered 1–16). Different toroidal cross-sections are shown by red lines and denoted by capital letters and numbers. The blue square is the location of the antenna.
(b) Poincaré plot of magnetic configuration and contours of magnetic field module at U-2M in antenna location. The circular line shows the vacuum chamber wall.
(c) General view of two-strap antenna in U-2M vacuum chamber. 1 and 2 straps, 3 antenna limiter.

OES - optical emission spectroscopy, VP - vacuum pumps, MS - mass spectrometer, MI - microwave interferometer, TP - triple probe.

Overview experiments

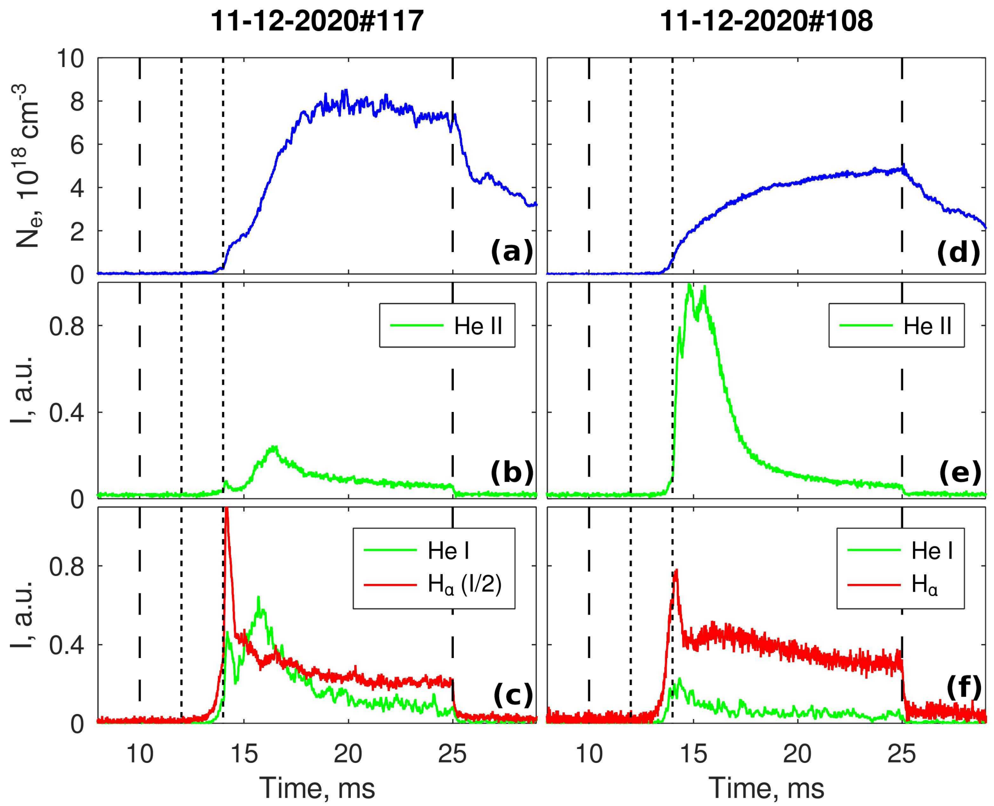

Time evolutions of average electron density N_e (a and d), optical emission intensities of ion He II (468.6 nm) (b and e), neutrals H I (H_α, 656.3 nm) and He I (447.15 nm) (c and f) for shots 11-12-2020#117 (p = 8.2×10^{-3} Pa) and 1-12-2020#108 (p = 2×10^{-3} Pa). The working gas content is ~ 26%H_2 +74%He. (f = 4.9 MHz, B_0 = 0.34 T, U_a = 8 kV). The vertical black lines indicate the times of duty cycle of RF shot.

The two-strap antenna operated in monopole phasing was used to produce the plasma.

To control RF power, the RF generator anode voltage U_a is varied stepwise as follows: $U_{a1} \approx 0.4\ U_a$ at the start, $U_{a2} \approx 0.6\ U_a$ at step 1, and the maximum anode voltage U_a was set at step 2.

At an anode voltage $U_a \approx 7$ kV, the RF power was ≈ 100 kW.

The RF frequency was equal to the fundamental hydrogen cyclotron harmonic $\omega_{RF} \approx \omega_{ci}\ (H^+) \approx 2\omega_{ci}\ (He^{2+}) \approx 4\omega_{ci}\ (He^+)$.

Y.V. Kovtun et al. Phys. Plasmas 31, 042501 (2024)

Overview experiments

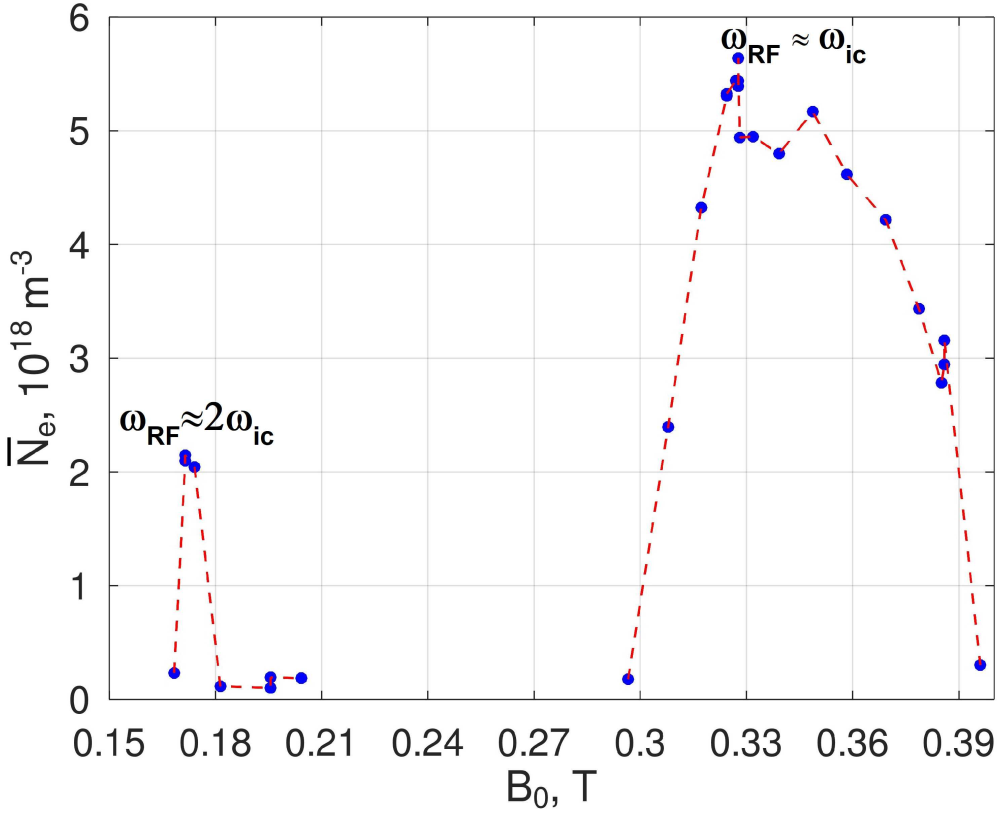

Average plasma density as a function of the value of magnetic fields. (f = 5 MHz, U_a = 6 kV, 16%H_2 +84%He, $p = 8.7\times10^{-3}$ Pa)

The maximum plasma density is observed in the range of $\omega_{RF} \approx \omega_{ci}$ (H^+). Increasing or decreasing the value of the magnetic field leads to a significant decrease in the plasma density by an order of magnitude.

The production of more dense plasma of ≈ 10^{18} m^3 is observed in the range of $\omega_{RF} \approx 2\omega_{ci}$ (H^+). However, the maximum plasma density is ≈ 2.8 times lower than in the case of plasma production at $\omega_{RF} \approx \omega_{ci}$ (H^+). As in the case of plasma production at $\omega_{RF} \approx \omega_{ci}$ (H^+), the plasma density decreases with increasing or decreasing magnetic field for the case of $\omega_{RF} \approx 2\omega_{ci}$ (H^+).

Y.V. Kovtun et al. Phys. Plasmas 31, 042501 (2024)

The ICRF plasma start-up (He+H_2 mixture)

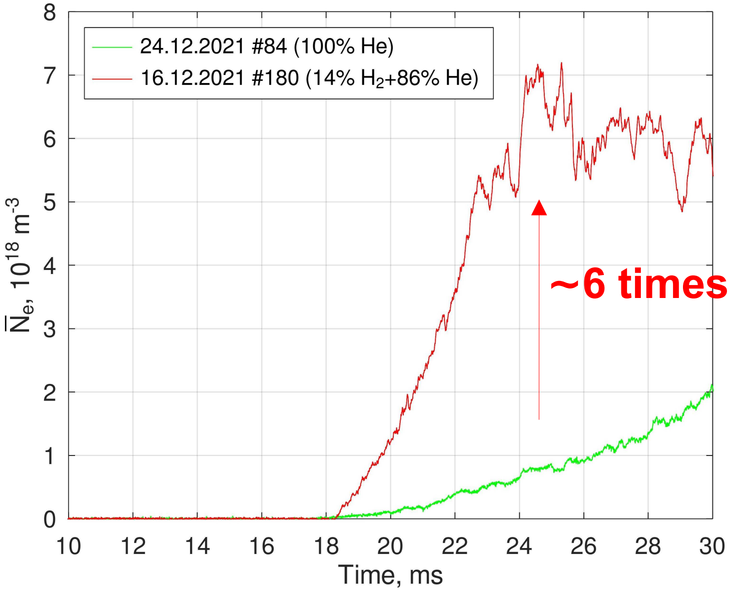

Time evolutions of average plasma density for **He** and gas mixture **14%H_2+86%He** for initial pressure p_0 = 3.4 × 10^{-2} Pa and U_a = 7 kV. (for He B_0 = 0.325 T, K_ϕ = 0.325, f = 4.96 MHz; for 14%H_2+86%He, B_0 = 0.32 T, K_ϕ = 0.34, f = 4.9 MHz).

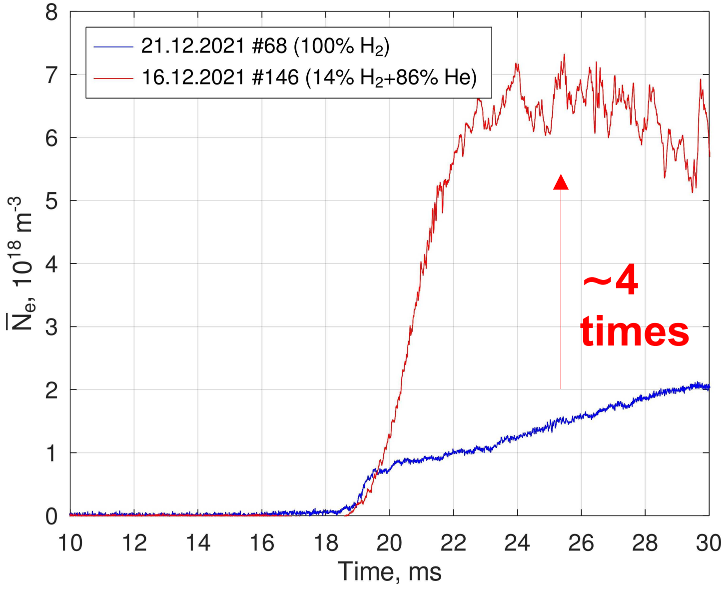

Time evolutions of average plasma density for **H_2** and gas mixture **14%H_2+86%He** for initial pressure p_0 =5 × 10^{-3} Pa and U_a = 7 kV. (for H_2 B_0 = 0.32 T, K_ϕ =0.34, f = 4.96 MHz; for 14%H_2+86%He, B_0 = 0.32 T, K_ϕ = 0.34, f = 4.9 MHz).

The plasma density achieved from the gas mixture is several times higher than from pure hydrogen and helium gases.

The dynamics of the plasma density increase is also different for the H_2+He and He.

Y. V. Kovtun, et al., Plasma Fusion Res. 18, 2402042 (2023)

Average plasma density (He+H_2 mixture)

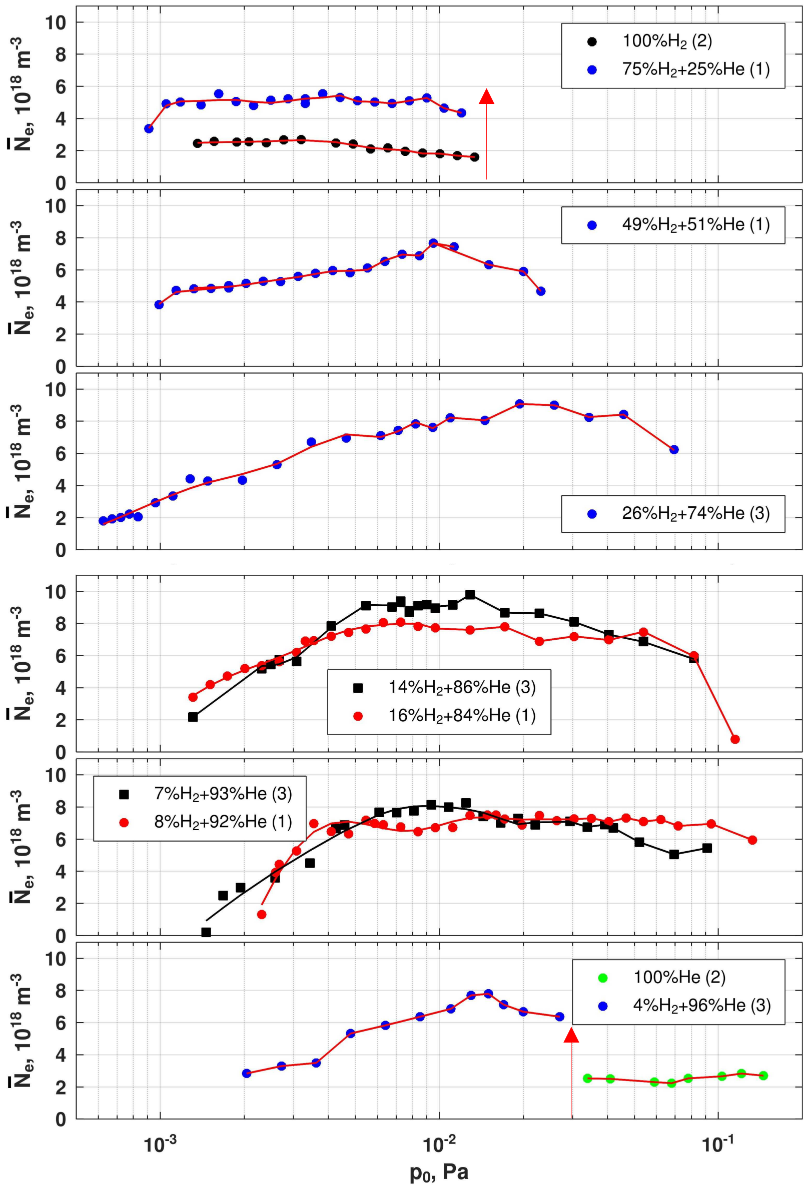

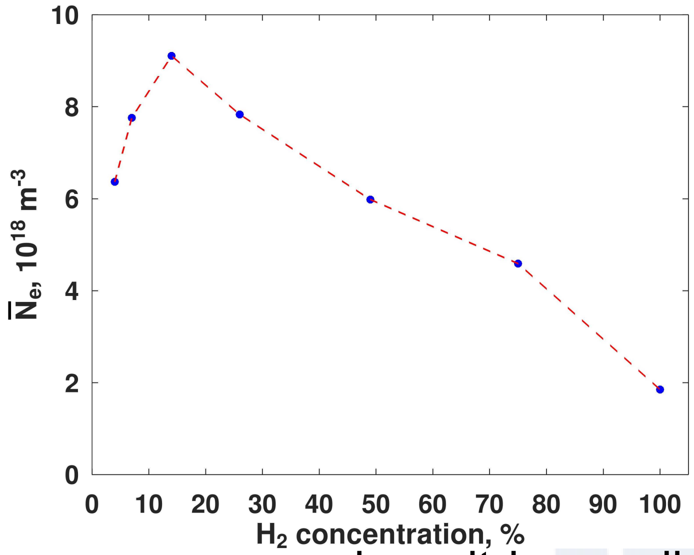

Average plasma density as a function of the of the initial hydrogen concentration in the mixture. (f = 4.9 MHz, U_a = 7 kV, p ~ 8×10^{-3} Pa)

The pressure range where it is possible to generate plasma with density higher than 10^{18} m^3 is wider in the He+H_2 mixture than in pure hydrogen and helium.

The plasma density as function of gas pressure has a broad maximum for each hydrogen concentration from the range 4-49%.

Average plasma density as a function of the pressure (1) [1] data of this experimental series, (2) and (3) experimental data [2, 3] and [4], respectively.
(f = 4.9 MHz, U_a = 7 kV)

1. Y. V. Kovtun, et al.,Phys. Plasmas 31, 042501 (2024)
2. Y. V. Kovtun, et al., Fusion Eng. Des. 194, 113887 (2023).
3. Y. V. Kovtun, et al., Plasma Fusion Res. 17, 2402034 (2022).
4. Y. V. Kovtun, et al., Plasma Fusion Res. 18, 2402042 (2023)

Electron and ion temperature

The case of pure helium and the helium–hydrogen mixture, the dependence has a general trend. Electron temperature increases as gas pressure decreases.

The maximum T_e is observed at the initial stage of $He+H_2$ plasma creation up to ≈ 40 eV. Further in time, the temperature decreases, and at 20ms, it is up to ≈ 15 eV in helium and up to ≈ 22 eV in the $He+H_2$ mixture.

The maximum temperature for He^+ ions was T_i ≈ 18 eV, and for C^+ ions, it was T_i ≈ 23 eV. Despite the fact that the initial hydrogen concentration in these experiments was different, the values of T_i were close.

Y.V. Kovtun et al. Phys. Plasmas 31, 042501 (2024)

Electron temperature

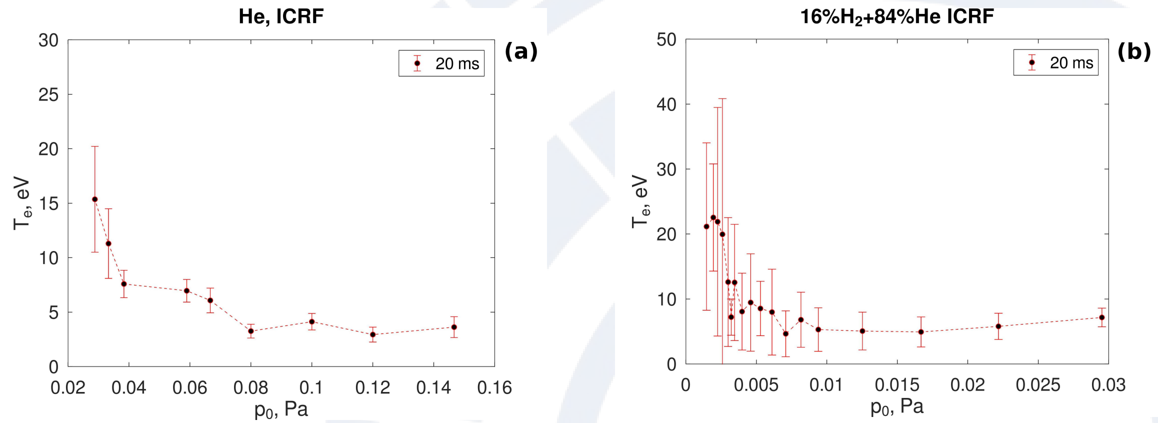

Average electron temperature as a function of the pressure in He (a) and 16%H_2 +84%He (b). (f = 4.9 MHz, U_a = 7 kV, B_0= 0.32 T).

Ion temperature

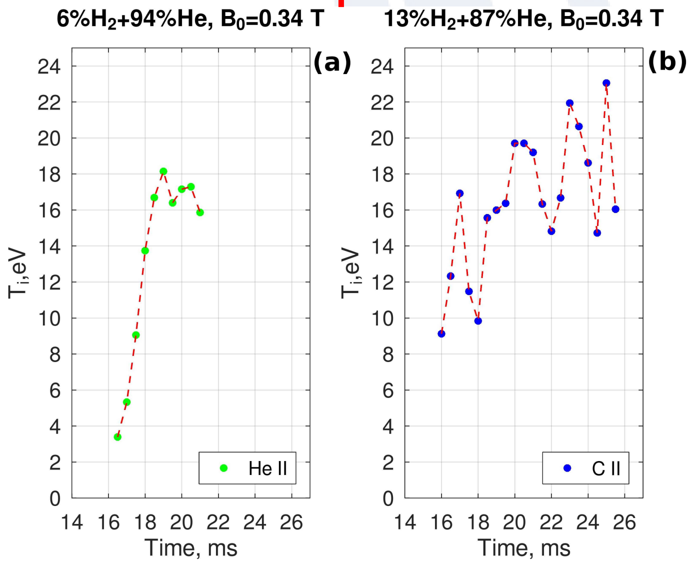

Time evolution of ions temperature He^+ (He II 468.6nm) (a) and C^+ (C II 426.7nm) (b) for p = 2.3×10^{-3} Pa (f = 4.9 MHz, U_a = 7 kV).

Supersonic molecular beam injection in helium and He+H plasma

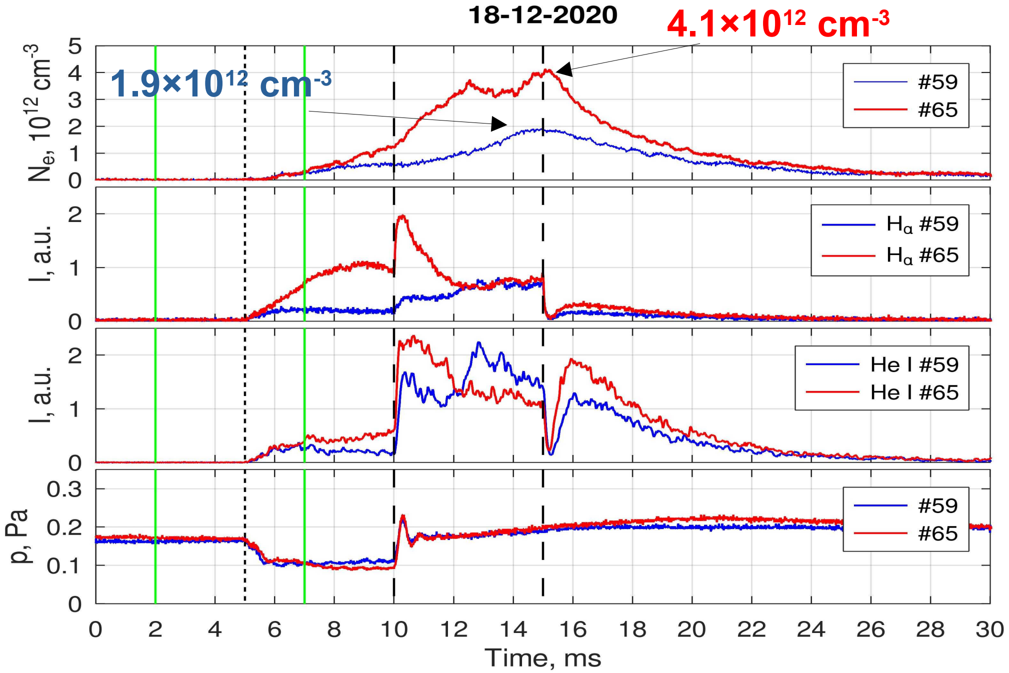

Time evolutions of average plasma density; optical emission intensities of H_α, (656.2 nm), He I (447.15 nm), and gas pressures.
(Frame antenna U_a= 4 kV, f=5 MHz, Two-strap antenna U_a=7 kV, f=4.92 MHz, B_0= 0.346 T, K_φ=0.324. Working gas He).

Duty cycle: Frame antenna 5 ms (start), 10 ms (shutdown); Two-strap antenna 10 ms (start), 15 ms (shutdown).

The vertical black lines indicate the times of duty cycle of RF shot. The vertical green lines indicate the times of duty cycle of gas injection.

The maximum average plasma density was increased from 1.9×10^{12} cm^{-3} in helium plasma to 4×10^{12} cm^{-3} after hydrogen injection. Accordingly, the density was increased by a factor of **2.1**.

Shots #59 without additional gas injection and # 65 with an additional injection of hydrogen gas.

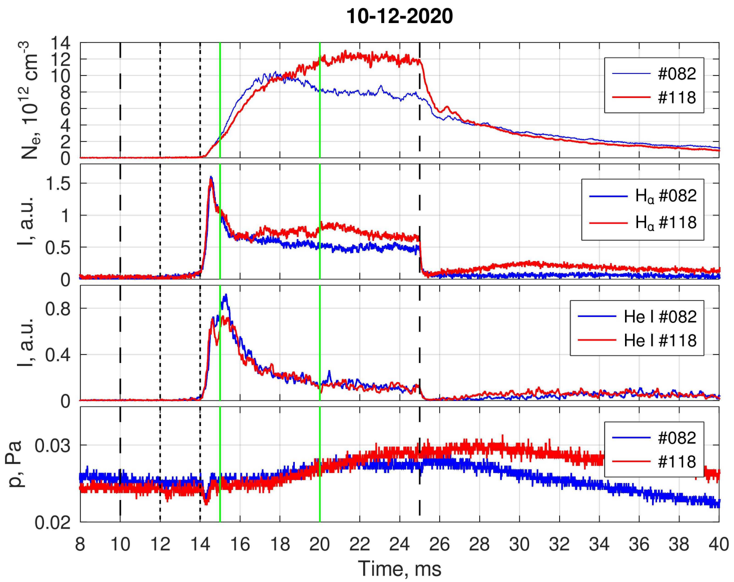

The maximum plasma density was observed to increase from 10×10^{12} cm^{-3} to 13×10^{12} cm^{-3} after SMBI injection. Accordingly, the density has been increased by **30%**.

Shots #082 without additional gas injection and # 118 with an additional injection of hydrogen gas.

Y.V. Kovtun et al. In: 49th EPS Conference on Plasma Physics, July 3 - 7 2023, Bordeaux, France.

ICRF production of plasma in He+H_2+D_2

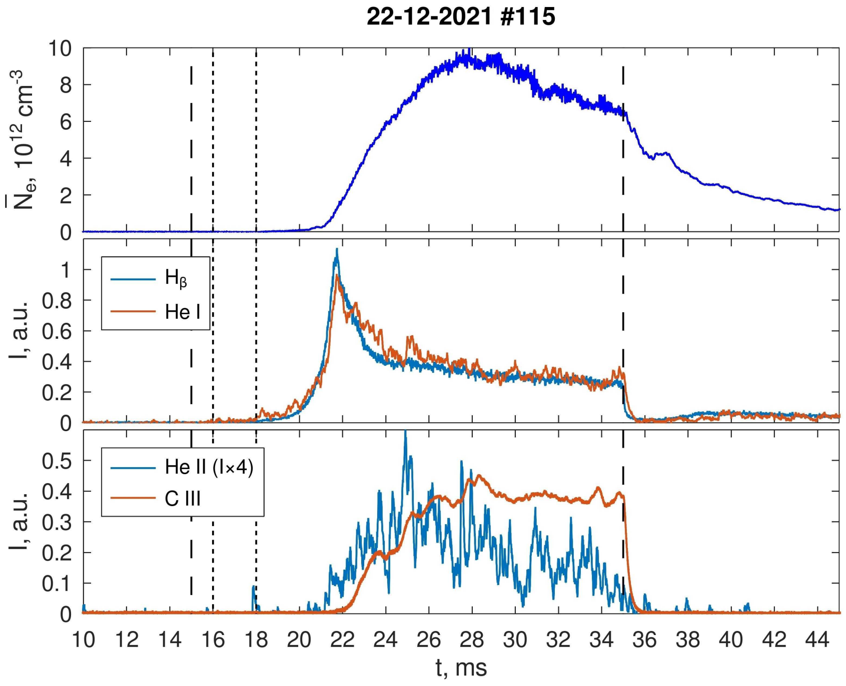

Time evolutions of average plasma density; optical emission intensities of H_β, (486.1 nm), He I (504.7 nm), and ions He II (468.6 nm); C III (464.7 nm), (U_a=7.5 kV, f=4.95 MHz, B_0=0.325 T, K_φ=0.33, I_{corr}=140A. Working gas 80% He+10%H_2+10%D_2, p = 9.7×10^{-2} Pa). Duty cycle: 15 ms (start), 16 ms (step-1), 18 ms (step-2), 35 ms (shutdown). The vertical lines indicate the times of duty cycle of RF shot.

Y. V. Kovtun, et al., Fusion Eng. Des. 194, 113887 (2023).

Thus, the investigation shows that the ICRF plasma production scenario developed for the He+H_2 mixture can be used in the He+H_2+D_2 mixture. The plasma parameters obtained in He+H_2+D_2 do not differ significantly from the plasma parameters in He+H_2.

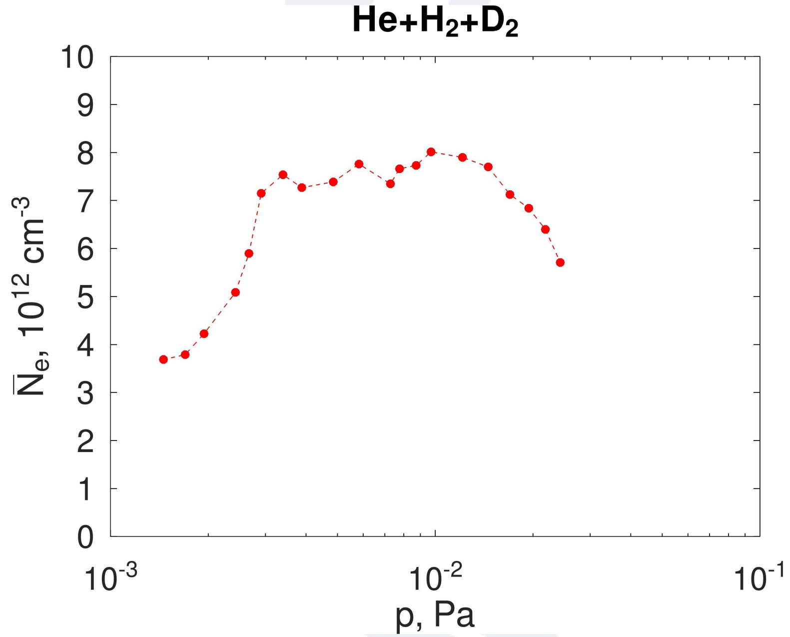

Maximum average plasma density as a function of the pressure. Working gas 80%He+10%H_2+10%D_2 (U_a=7 kV, f=4.95 MHz, B_0=0.323 T, K_φ=0.32, I_{corr}=157A).

ICRF production of plasma in Ar+H_2

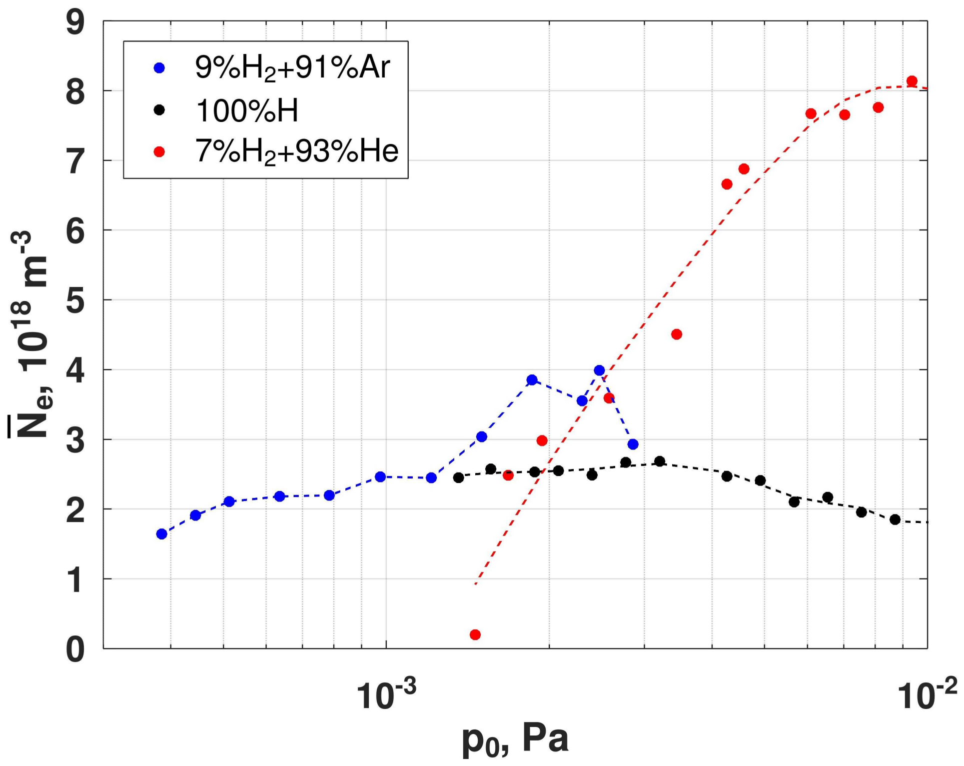

Comparision of average plasma density as a function of the pressure (Ua = 7 kV, f = 4.9 MHz) for 9%H_2+91% Ar (B_0 = 0.33 T), 100%H_2 (B_0 = 0.324 T) [2], 7%H2+93%He (B_0 = 0.35 T) [3].

Plasma production with an average plasma density up to ~ 4×10^{18} m^{-3} was observed. The plasma density obtained in the argon-hydrogen mixture is higher than in pure hydrogen which is characteristic.

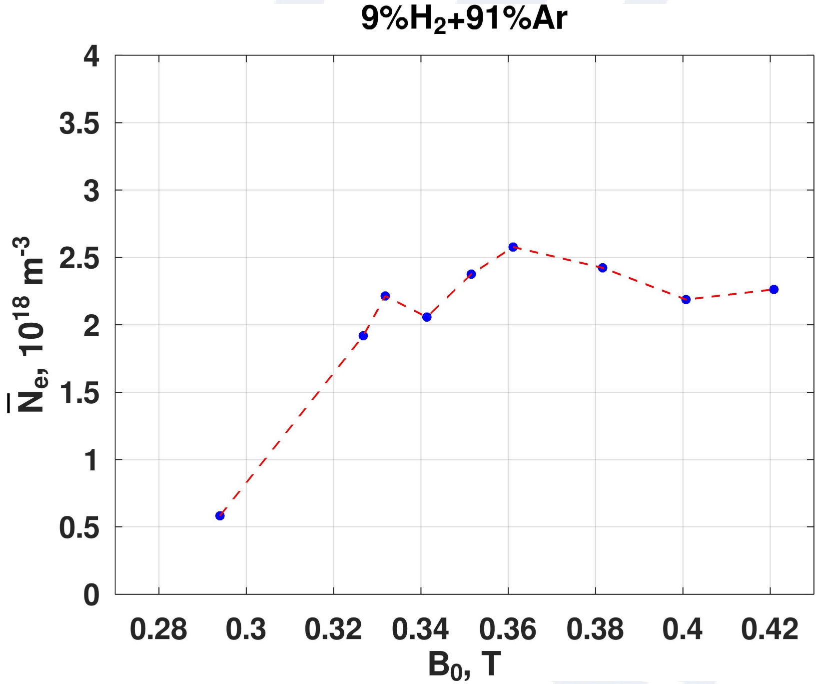

Average plasma density as a function of the value of magnetic fields (f = 4.9 MHz, Ua = 6 kV, 9%H_2+91% Ar, and p = 2.1 10^{-3} Pa).

1. Y. V. Kovtun, et al., in 24th International Stellarator Heliotron Workshop 9-13 September 2024, Hiroshima, Japan. ID 70.
2. Yu.V. Kovtun et al. Plasma Fusion Res. 2023, 18, 2402042.
3. Yu.V. Kovtun et al. Plasma Fusion Res. 2022, 17, 2402034.

Minority ICRF plasma production scenario

- Plasma is produced by gas ionization by electron impact;
- Electron plasma component is heated by the slow wave (SW);
- At low plasma densities it is heated by SW directly excited by the antenna. Since the power needed is low, good antenna coupling to the SW is not necessary;
- At higher densities, the fast wave excited by the antenna converts to the SW at the Alfvén resonance layer. The SW propagates towards the lower hybrid resonance layer, where it is fully absorbed.

1. V. Moiseenko et al. J. Plasma Phys., 86, 905860517 (2020).

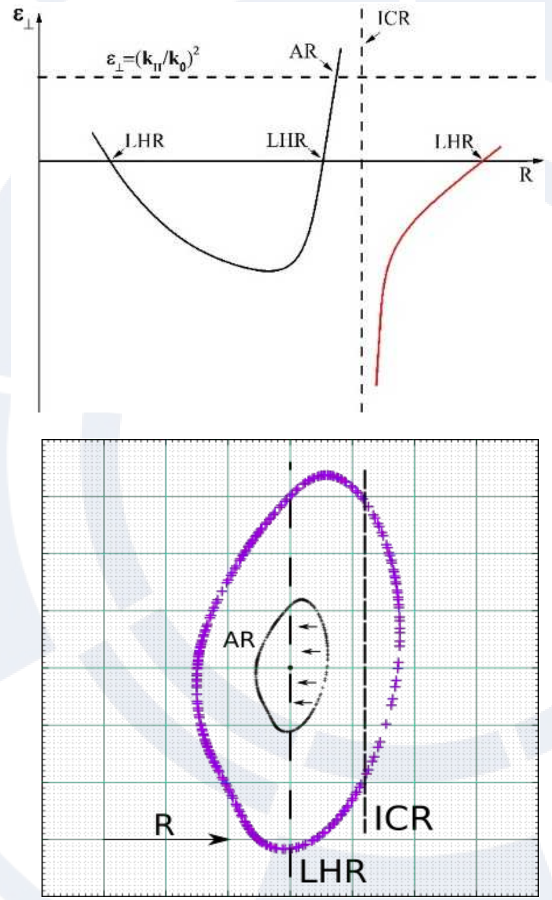

Sketch illustrates FM-SW conversion into SW in the presence of a minority inside the plasma column. [1]

Propagation of electromagnetic waves

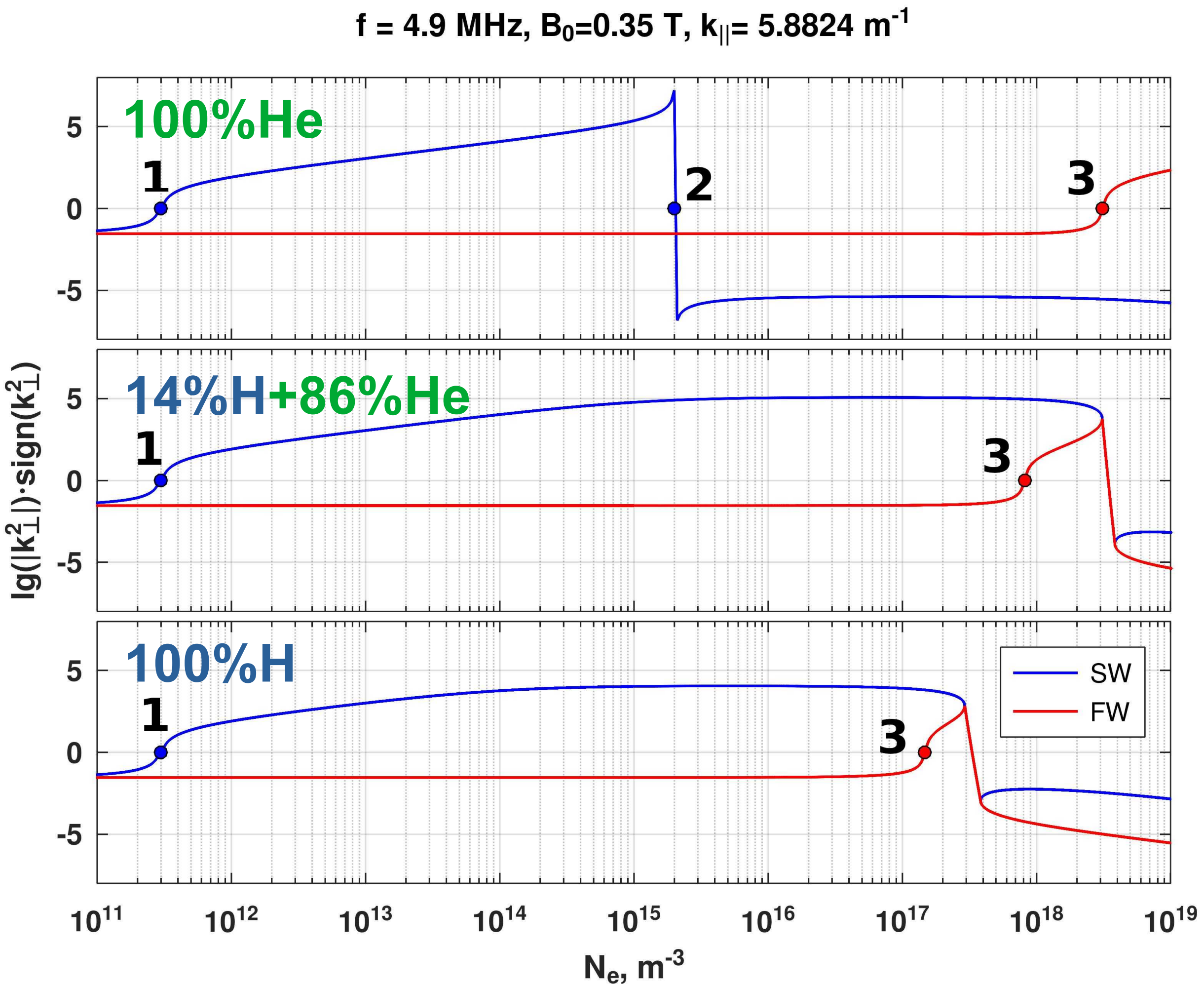

The squared perpendicular wave numbers of slow waves (SW) and fast waves (FW) of 4.9 MHz frequency as a function of the plasma density, in He, He+H mixture, and H. The numbers correspond to 1 - cutoff SW, 2 - lower hybrid resonance, and 3 - cutoff FW.

The minimum critical density above which **SW** can propagate is determined from the relation ($k_{\perp,SW} = 0$):

$$\omega_{RF}^2 = \omega_{pe}^2 + \omega_{pi}^2, \ (1)$$

The upper limit of plasma density above which **SW** do not propagate for cold plasma is determined by the condition of lower hybrid resonance ($k^2_{\perp,SW} \rightarrow \infty$):

$$\omega_{RF}^{\ 2} = \omega_{LH}^2, \ (2)$$

For an **FW**, the plasma density threshold is determined by the cutoff FW at $k_{\perp,FW} = 0$.

$$\omega_{pi}^{\ 2} = (N^2_{||} - 1)\, \omega_{ci}\, (\omega_{RF} + \omega_{ci}), \ (3)$$

Further increase in the plasma density leads to the FW conversion to SW at the conversion point (Alfven resonance) [1-3].

1. V. Moiseenko et al. J. Plasma Phys., 86, 905860517 (2020).
2. R. Klima, A. V. Longinov, and K. N. Stepanov, Nucl. Fusion 15, 1157 (1975).
3. Y.V. Kovtun et al. Phys. Plasmas 31, 042501 (2024)

Summary of results at U-2M

Experiments on ICRF plasma production in the He+H_2 mixture with initial hydrogen concentration up to 75% at U-2M have indicated that:

(i) the plasma density achieved from the gas mixture is several times higher than from pure hydrogen and helium gases in the investigated range of hydrogen concentration,

(ii) plasma with a density higher than 10^{18} m^3 was produced when the RF frequency was close to the fundamental hydrogen cyclotron harmonic $\omega_{RF} \approx \omega_{ci}$ (H^+),

(iii) the plasma density depends on the hydrogen concentration, and the densest plasma is observed at an initial concentration of 14% hydrogen in the mixture,

(iv) the electron temperature depends on the initial pressure in the mixture and was low to ≈ 5–40 eV,

(v) the maximum ion temperature was up to ≈ 18–23 eV,

(vi) is possible realization of this scenario on He+H_2+D_2 and Ar+H_2 mixture.

However, the U-2M is notably smaller than Large Helical Device (LHD) and W7-X. Moreover, the magnetic fieldin U-2M is an order of magnitude lower.

ICRF production of plasma in Large Helical Device

Large Helical Device (LHD)

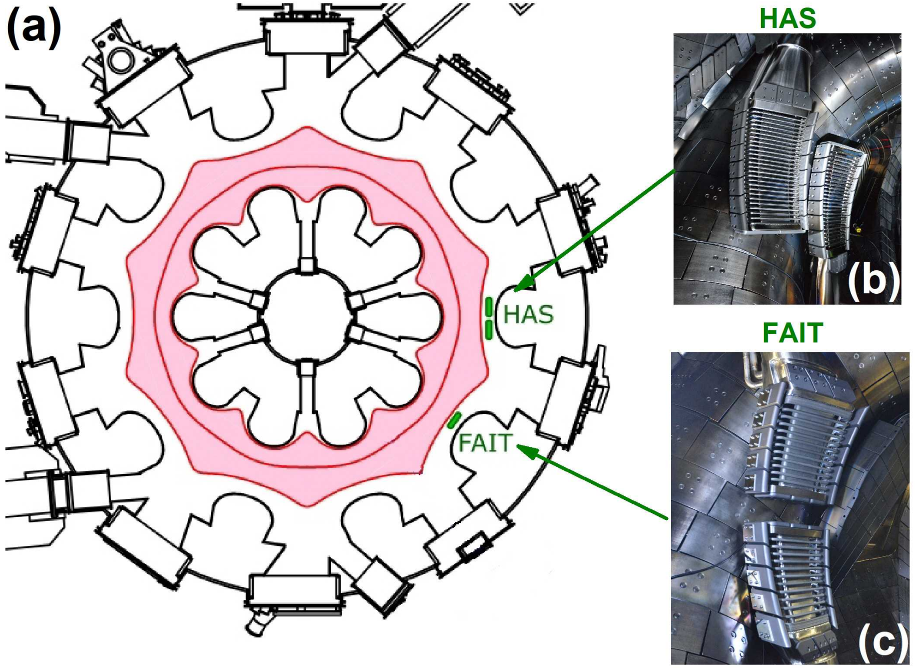

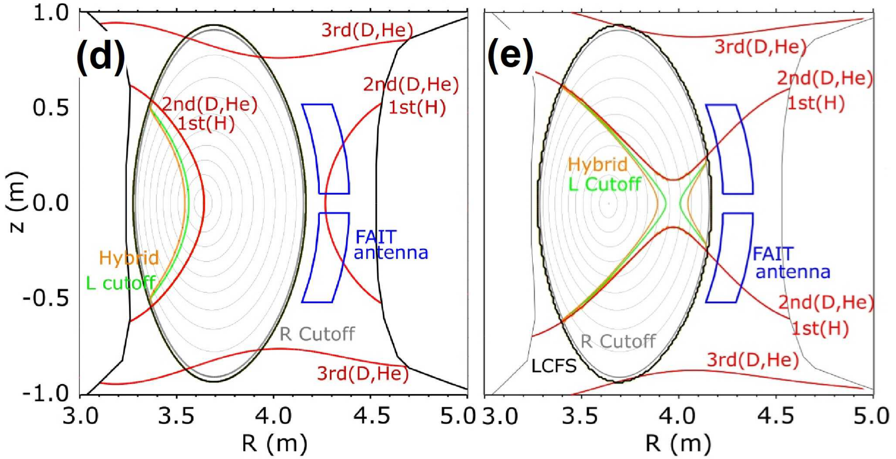

The LHD is a large-scale heliotron-type superconducting device at Toki, Japan [1].

Device characteristics	
Major radius, R (m)	**3.9**
Minor radius, r (m)	**0.6**
Plasma volume, V_p (m^3)	**~ 30**
Magnetic field, B (T)	**3**
Total heating power, (MW)	**36**
Plasma heating tools	**ECRH, NBI, ICRF**

1. **Iiyoshi A. et al (1999) Nucl. Fusion 39 1245**

(a) Schematic view of the mid-plane cross-section of LHD.
(b) General view of HAS antenna in LHD vacuum chamber.
(c) General view of FAIT antenna in LHD vacuum chamber.
LHD cross-section at FAIT antenna location. Last closed flux surface, magnetic surfaces, ion cyclotron resonance layers for R_{ax} = 3.6 m,
(d) B_t = 2.55 T, and
(e) B_t = 2.75 T.

ICRF at LHD

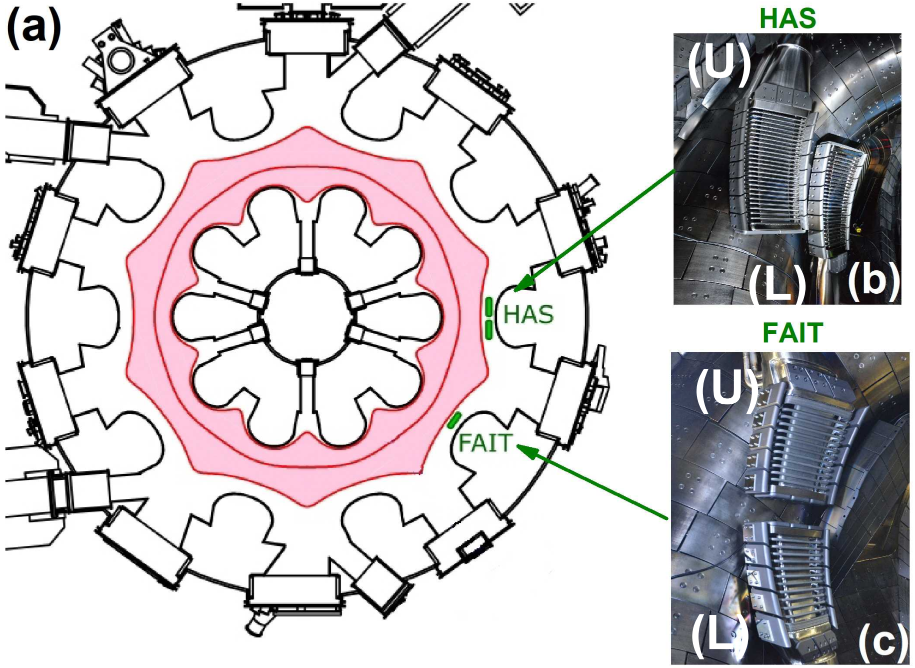

The ICRF heating is used with a fixed frequency of 38.47 MHz [1]. The maximum output power is 3 MW.

There are two types of antennas on the LHD:
a Hand-Shake form antennas (HAS) [2] and
a Field-Aligned-Impedance Transforming (FAIT) antennas [3].

The HAS and FAIT antennas are located at ports 3.5 and 4.5, respectively. The antennas occupy the upper (U) and lower (L) ports of the LHD vacuum chamber. All the straps are shielded by the Faraday screens.

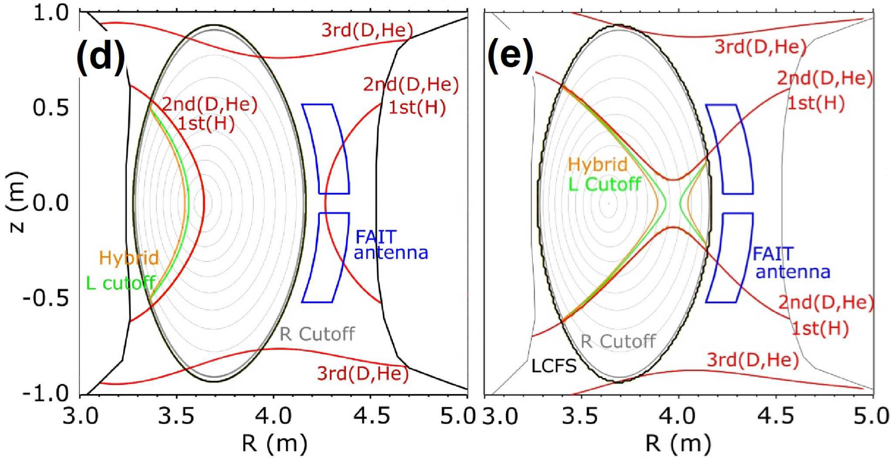

1. Kamio S. et al (2022) Nucl. Fusion 62 016004
2. Kasahara H. et al (2011) 38th EPS Conf. Plasma Physics vol 35G p P2.099
3. Saito K., et al. (2015) Fusion Eng. Des. 96–97 583

(a) Schematic view of the mid-plane cross-section of LHD.
(b) General view of HAS antenna in LHD vacuum chamber.
(c) General view of FAIT antenna in LHD vacuum chamber.
LHD cross-section at FAIT antenna location. Last closed flux surface, magnetic surfaces, ion cyclotron resonance layers for R_{ax} = 3.6 m,
(d) B_t = 2.55 T, and
(e) B_t = 2.75 T.

ICRF plasma start-up in helium–hydrogen mixtures. First results.

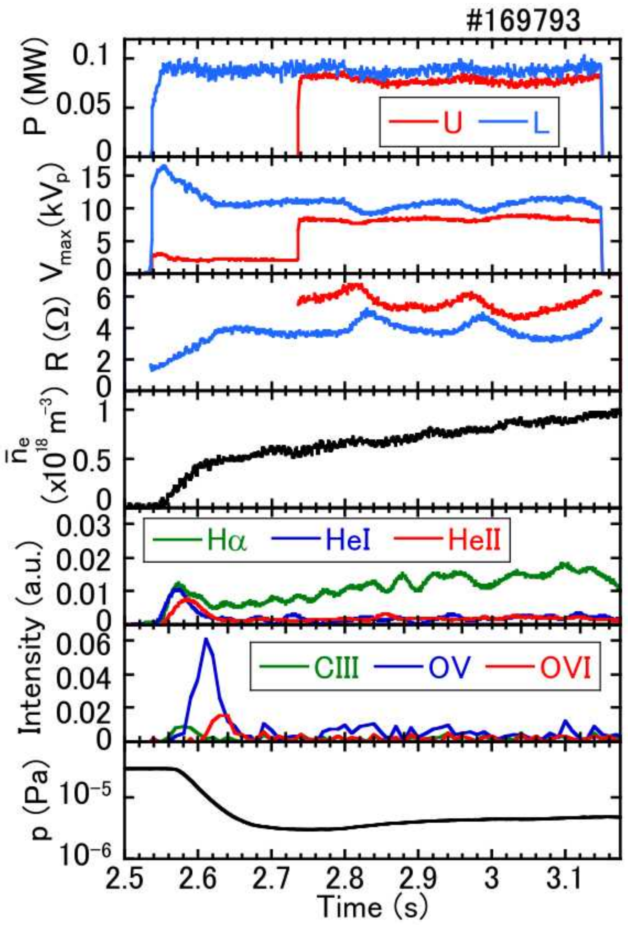

Time evolutions of ICRF power P_{ICRF}, (antennas FAIT U and L), maximum voltage at the coaxial line V_{max}, loading resistances R, average electron density ne, optical emission intensities of Hα (656.3 nm), HeI (587.6 nm), HeII (468.6 nm), CIII (97.7 nm), OV (63 nm) and OVI (103.4 nm), and neutral gas pressure p. Working gas content is ~81% He + 19% H_2.

In those experiments, the ICRF plasma production was for the first time demonstrated using the field-aligned antennas. The plasma has a low density, but can serve as target plasma for NBI.

The major constraint of the experiments is the low RF power. As a result, the low plasma density is obtained, and the antenna-plasma coupling was not high. Also, the full ionization of neutral gas was not achieved.

S. Kamio, V.E. Moiseenko, Yu. V. Kovtun et al. Nucl. Fusion 61, 114004 (2021)

ICRF plasma start-up in helium–hydrogen mixtures.

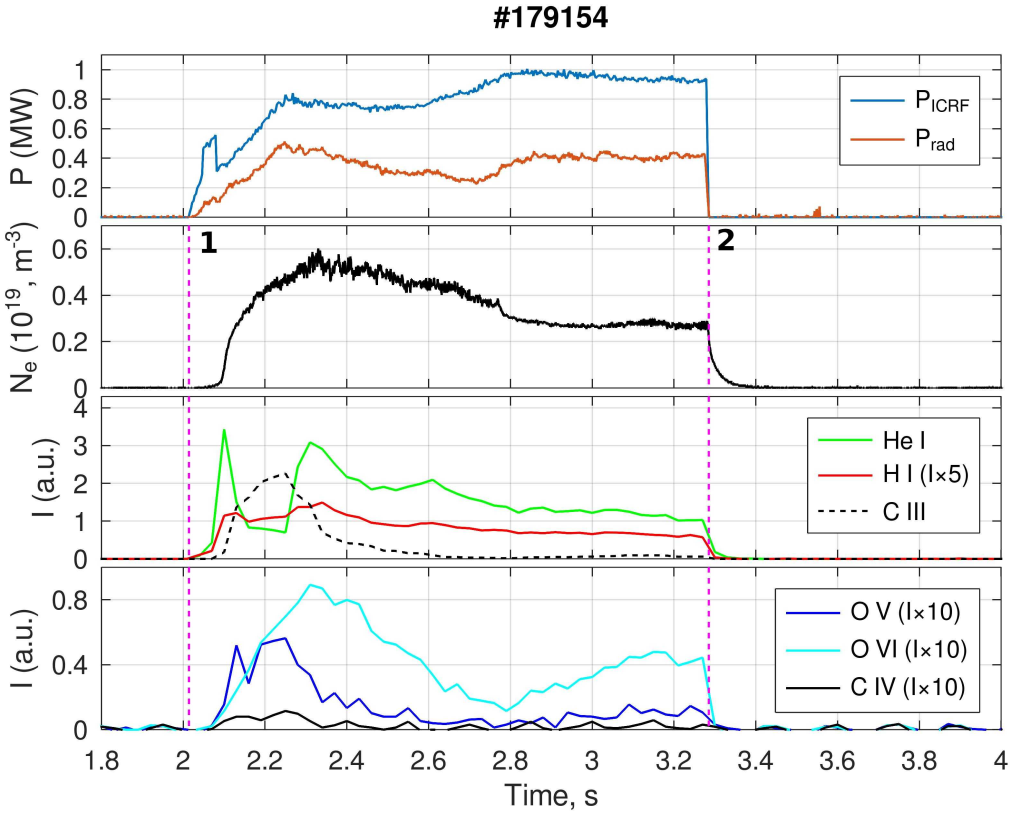

Time evolutions of injection power P_{ICRF} (total), radiation power P^{rad}, average electron density N_e, optical emission intensities of H I (H_α 656.3 nm), He I (587.6 nm), C III (97.7 nm), O V (63 nm), O VI (103.4 nm), and CIV (154.9 nm). Dashed dotted lines denote: switch-on RF (1), switch-off RF (2). The working gas content is ~22.5% H_2 + 77.5% He. B_0 = 2.75 T [2].

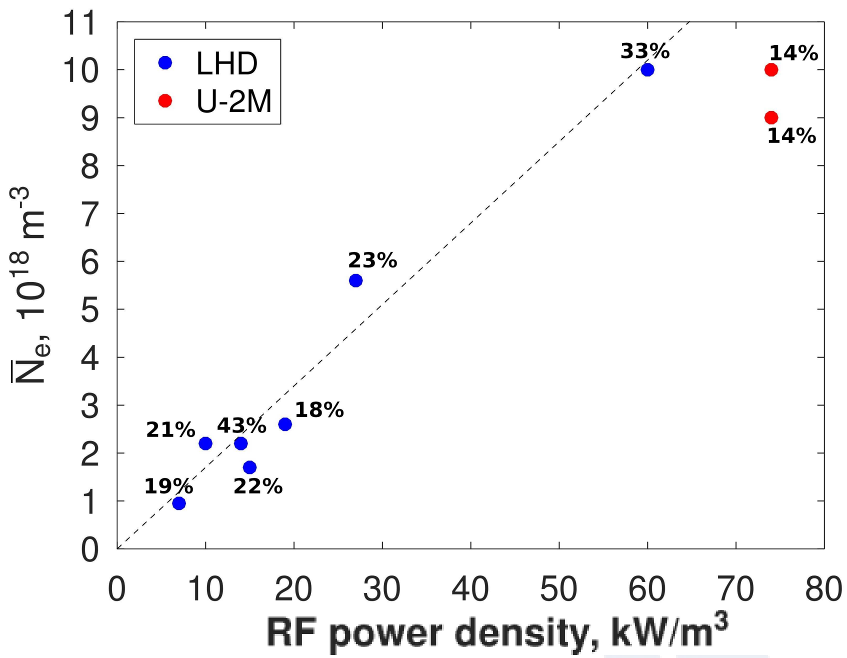

Dependence of maximum plasma density on RF power density in LHD and U-2M. The percentage values near the dots correspond to the initial concentration of hydrogen in the gas mixture H_2+He [1].

Increase of the RF power predictably results in increase of the density of produced plasma. Without pre-ionization the plasma density achieved in shot #179154 is 6×10^{18} m^{-3} which 6 times more than in previous experiments.

Experiments on U-2M and LHD have shown that RF power density at the level or more than 60 kW/m^3 is necessary to produce a plasma with relatively high density 10^{19} m^3.

1. Y. V. Kovtun, et al., Plasma Fusion Res. 18, 2402042 (2023)
2 Yu.V. Kovtun et al 2023 Nucl. Fusion 63 106002

ECR+NBI+ICRF in helium–hydrogen mixtures.

The ECR+NBI+ICRF scenarios allow RF heating of both the electron and ion components of the plasma is possible.

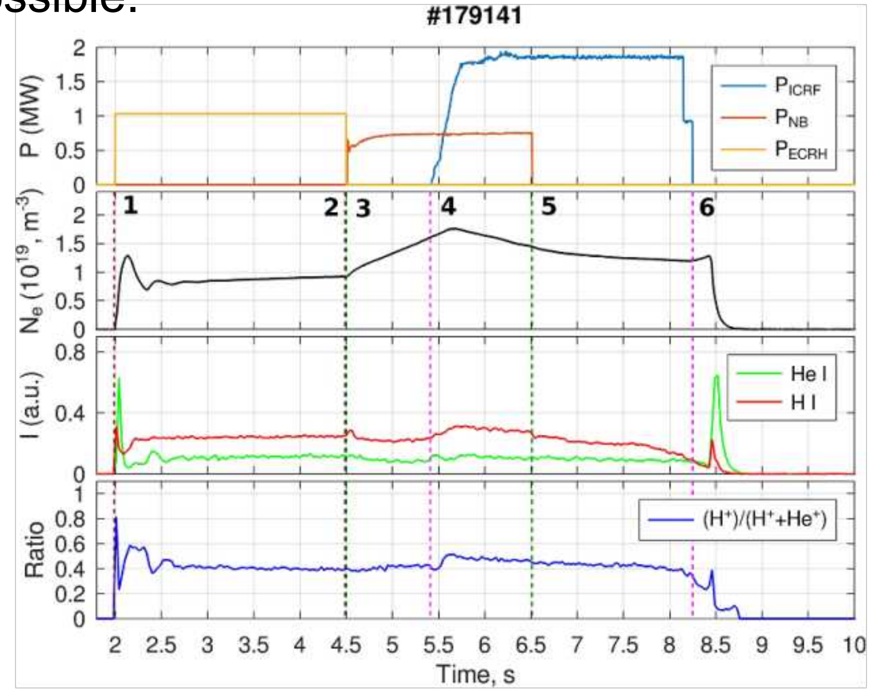

Time evolutions of injection powers P_{ICRF} (total), P_{NB} and P_{ECRH}, average electron density N_e, optical emission intensities of H I (H_α 656.3 nm), He I (587.6 nm) and percentage of hydrogen. Dashed dotted lines: switch-on ECRH (1), switch-off ECRH (2) switch-on NB (3), switch-on RF (4), switch-off NB (5), switch-off RF (6). The working gas content is ~22.5% H_2 + 77.5% He. B_0 = 2.75 T.

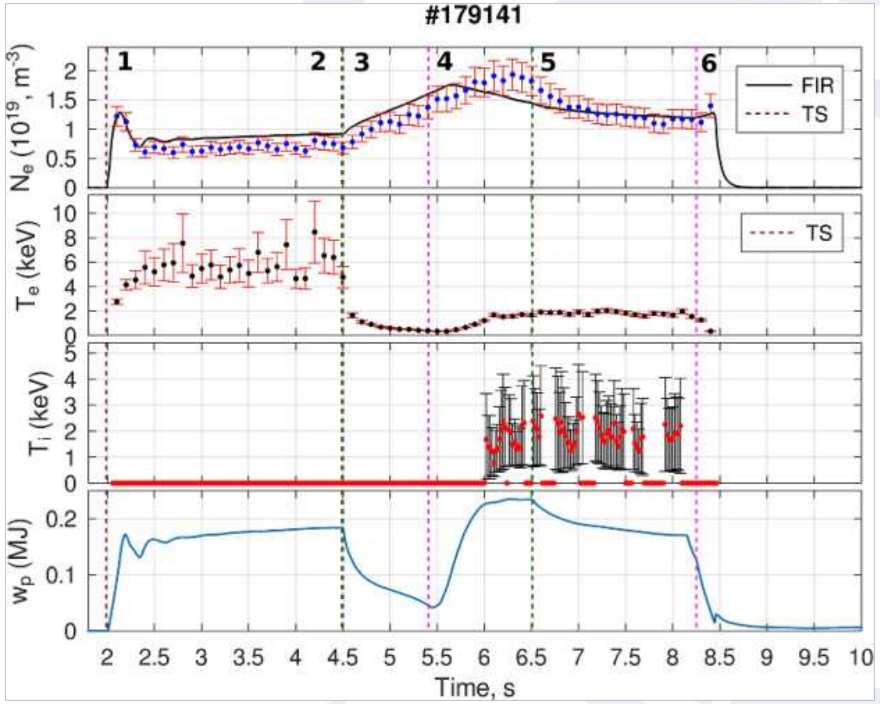

Time evolutions of average electron density N_e, electron temperature T_e, ion temperature T_i and plasma energy content w_p. Dashed dotted lines: switch-on ECRH (1), switch-off ECRH (2) switch-on NB (3), switch-on RF (4), switch-off NB (5), switch-off RF (6). The working gas content is ~22.5% H_2 + 77.5% He. B_0 = 2.75 T, FIR (R = 3.669 m), TS (R = 3.602 m)

Yu.V. Kovtun et al 2023 Nucl. Fusion 63 106002

ICRF plasma production and heating in LHD. First results (I).

continuous mode of gas fueling

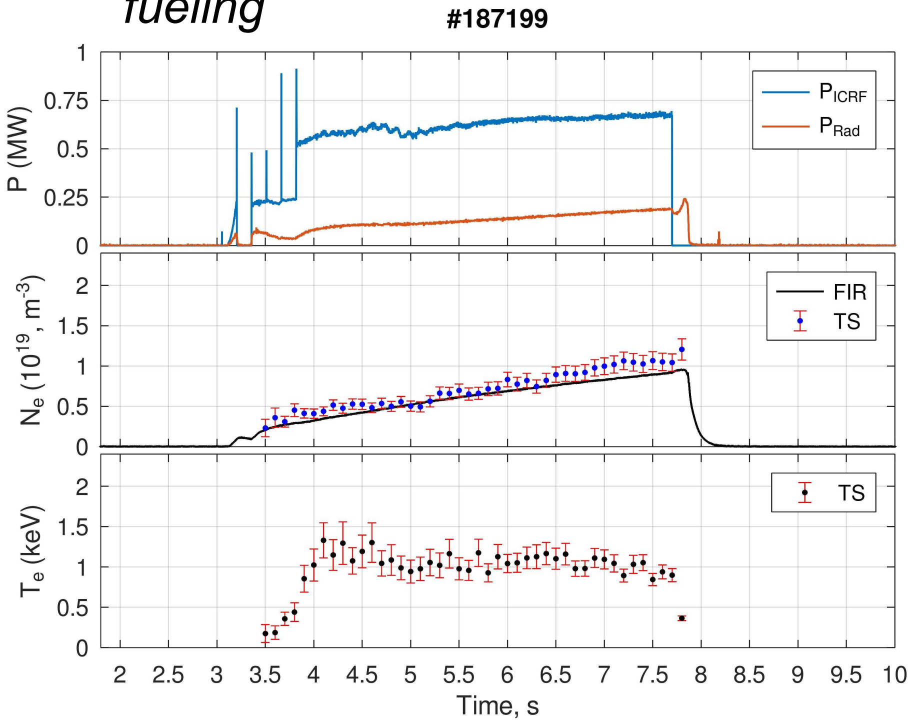

Time evolutions of RF power P_{ICRF} (total), radiation power P_{rad}, electron density N_e, and electron temperature Te in continuous gas puff mode for the LHD discharge #187199. The average electron density of far-infrared (FIR) laser interferometer at R = 3.669 m, electron density and temperature of Thomson scattering (TS) at R = 3.602 m are given. The initial working gas content is ~30% H_2 + 70% He.

pulsed mode of gas fueling

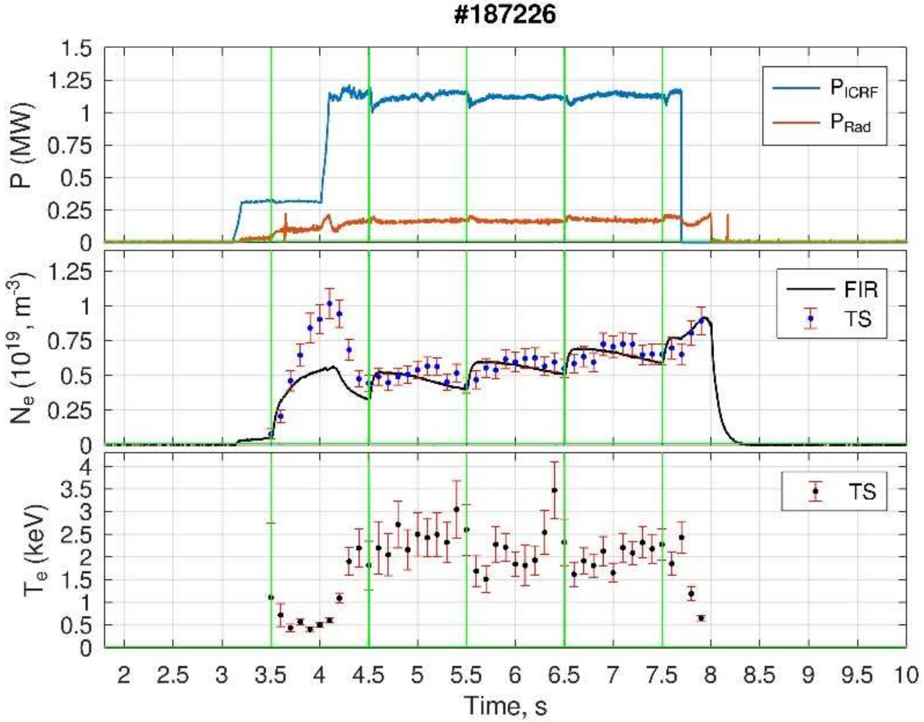

Waveforms of the injected power P_{ICRF} (total), radiation power P_{rad}, electron density N_e, and electron temperature T_e in with pulsed gas supply. The vertical green lines indicate gas puff moments. The data average electron density of far-infrared (FIR) laser interferometer at R = 3.669 m, electron density and temperature of Thomson scattering (TS) at R = 3.602 m are given. The initial working gas content is ~24% H_2 + 76% He.

V. E. Moiseenko, et al. Phys. Plasmas 32, 030701 (2025)

ICRF plasma production and heating in LHD. First results (I).

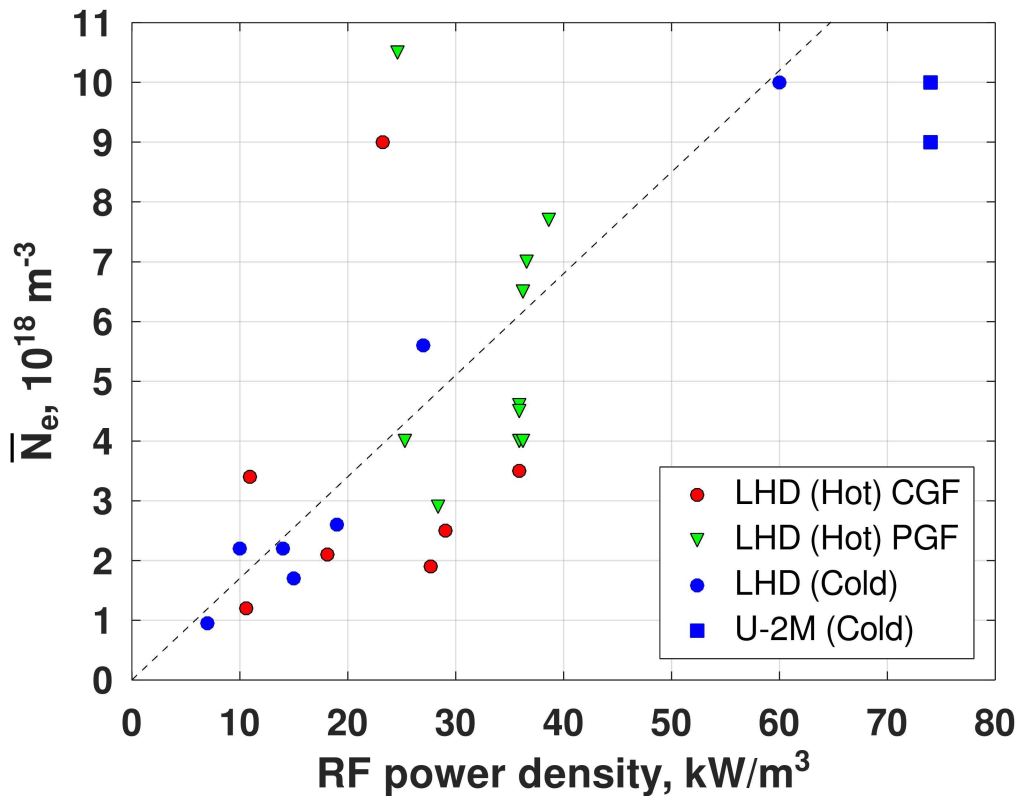

Dependence of maximum plasma density on RF power density in LHD and U-2M.

LHD(Cold) and U-2M(Cold) T_e < < 100 eV

LHD(Hot) T_e > > 100 eV

LHD(Hot)CGF continuous mode of gas fueling

LHD(Hot)PGF pulsed mode of gas fueling

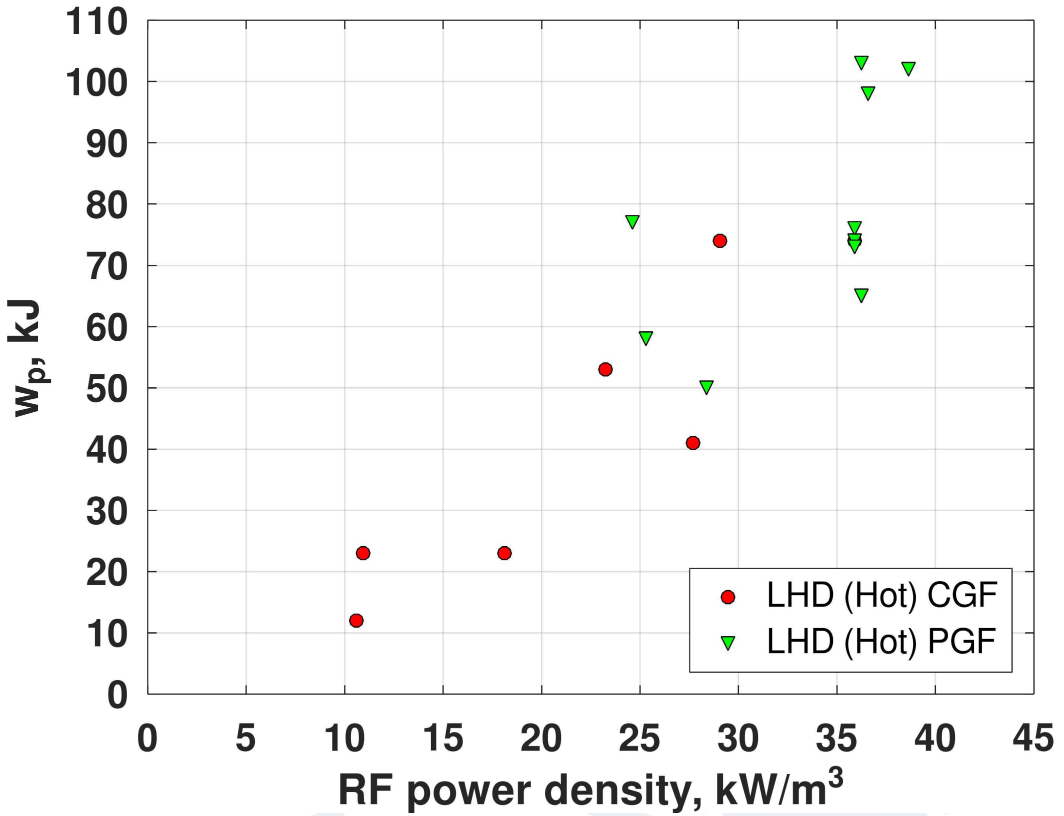

Dependence of maximum plasma energy content on RF power density in LHD.

LHD(Hot) T_e > > 100 eV

LHD(Hot)CGF continuous mode of gas fueling

LHD(Hot)PGF pulsed mode of gas fueling

ICRF plasma production and heating in LHD (II).

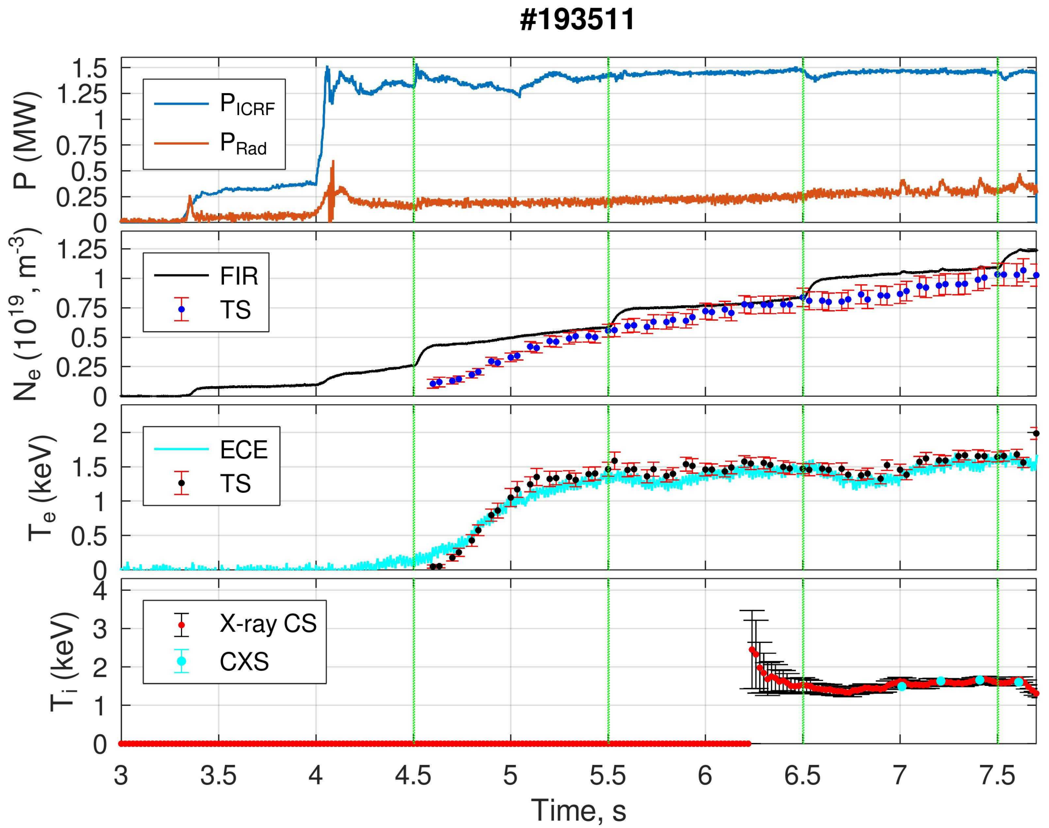

Time evolutions of injection power P_{ICRF} (total), radiation power P_{rad}, electron density N_e, electron temperature T_e and ions temperature T_i. The data of far-infrared (FIR) laser interferometer, R = 3.669 m, Thomson scattering (TS), R = 3.675 m and Electron cyclotron Emission (ECE), R = 3.67 m are given. X-ray crystal spectrometer (X-ray CS) Doppler-broadened ArXVII. Charge Exchange Spectroscopy (CXS), R = 3.64 m. Dashed dotted green lines: switch -on and - off gas puff He.

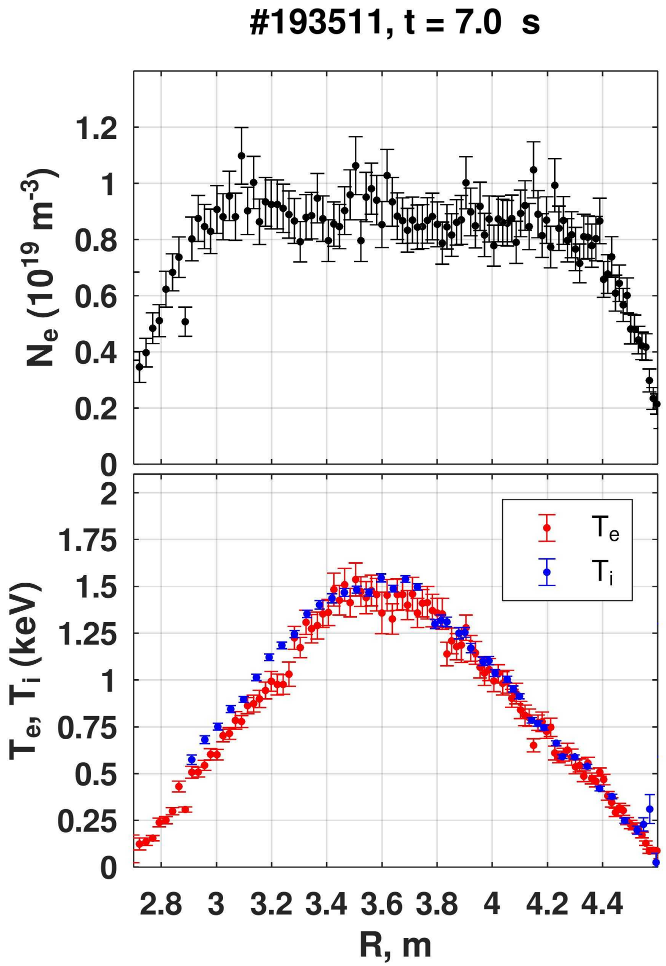

Comparison of the radial distribution of electron and ion temperature.

plasma density in some shots was higher than 1×10^{19} m^{-3}.

maximum electron temperature at the center was up to 2.5 keV.

maximum ion temperature was observed up to 2-3 keV.

ICRF plasma production and heating in LHD (II)

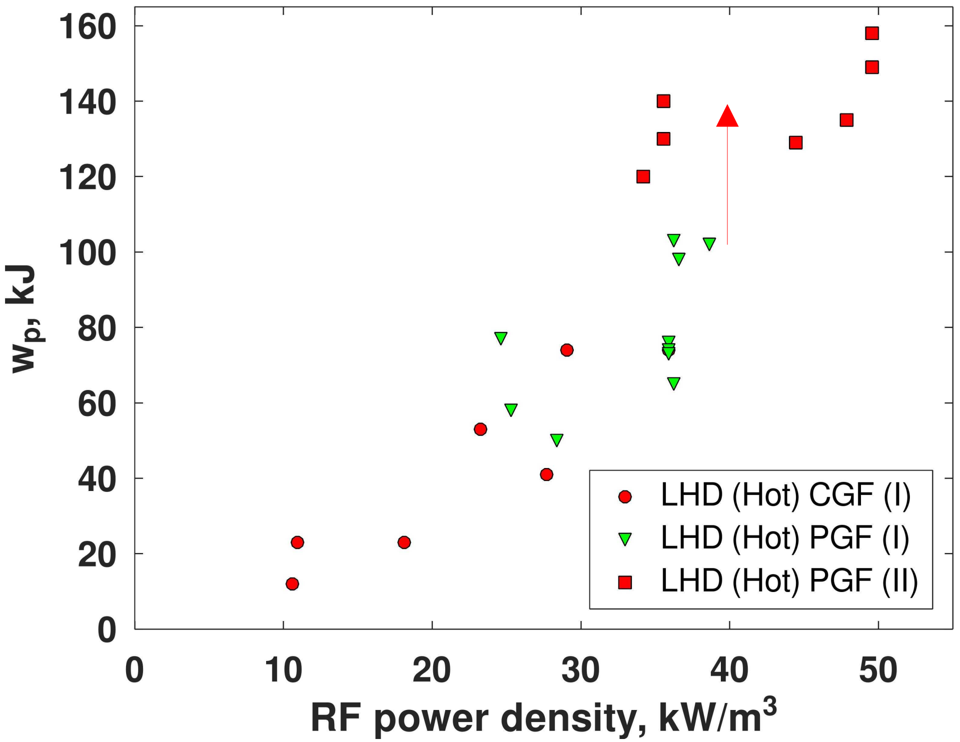

Dependence of maximum plasma energy content on RF power density in LHD.

LHD(Hot) $T_e >> 100$ eV
LHD(Hot)CGF continuous mode of gas fueling
LHD(Hot)PGF pulsed mode of gas fueling
I and II — first and second series of experiments

In the second series of experiments, higher values of plasma energy content were achieved compared to the first series of experiments.

The maximum plasma energy content was up to ≈ 158 kJ.

Summary of results at LHD.

Experiments on ICRF plasma production in the He+H_2 mixture at LHD have indicated that:

(i) the ICRF plasma start-up scenario developed at the U-2M can be scaled up on large helical devices,

(ii) stable breakdown and plasma production is observed,

(iii) two modes of plasma production can be realized: first producing a cold plasma that can be used for a wall conditioning procedure, and second producing and heating the plasma,

(iv) the maximum plasma density ion was up to ≈ 1×10^{19} m^{-3},

(v) the maximum electron temperature was up to ≈ 2–2.5 keV,

(vi) the maximum ion temperature was up to ≈ 2-3 keV,

Summary

To conclude, the demonstrated startup scheme opens possibilities to develop different plasma production-heating scenarios in ICRF for stellarators that complement ECRH scenarios, significantly enhancing accessible plasma settings such as the magnetic field strength (given the fixed frequencies of resonance heating or the application of neutral beam injection).

The point out two unique advantages: (i) ICRF startup does not have any upper plasma density limit, and (ii) for stellarators having high magnetic fields, ICRF generators are available at an affordable price. Gyrotrons for X2 operation at high magnetic fields (potentially for reactor scale devices), however, are not yet developed.

For future improvements for ICRH plasma production, the extended experience accumulated on tokamaks will be useful.

Thank you for your attention and time